

# Sensing and Control for Geometry Stability of the Melt Pool and the Cross Sectional Area in Laser Cladding

Liangliang Nan and Weijun Liu

*Shenyang Institute of Automation, Chinese Academy of Sciences, Shenyang, Liaoning Province, China*

*{nanliang & wjliu}@sia.cn*

Liangliang Nan

*Graduate School of the Chinese Academy of Sciences, Chinese Academy of Sciences, Beijing, China*

*nanliang@sia.cn*

## Abstract

*The accurate control of process parameters is particularly important for the growth of high quality structures during laser cladding. Melt pool size and cross sectional area are key process characteristics that can be controlled to allow the precise deposition of complex features. A feasible mathematical model is established to describe the interaction between laser and powder particles and to predict and control the cross sectional area. Also, a vision-based sensing system is proposed to detect the transient shape and size of the melt pool. The system focuses on the measuring of the geometric parameters of the melt pool by using a digital image processing method and thus giving researchers the parameters on-line, which gives us a necessary tool to gain insight into the cladding process and to optimize the material quality.*

## 1. Introduction

Laser cladding is rapidly gaining importance. It refers to advanced laser-based fusion processes used to add features to an existing part, and a means for more efficient part manufacture or part repair. Because of the advantages, such as local heating, possibility to automate and applicability to dissimilar materials, laser cladding has been widely used to produce high quality surface layers on top of new parts, to produce entire parts, and to refurbish and to improve used parts.

Since laser cladding is a high precision and complicated process, in order to achieve much better results, such as geometric accuracy and surface roughness, a great number of experiments must be performed to select process parameters appropriately. However, the cladding process involves multiple process parameters that are strongly coupled with each

other and their effects are still far from being completely understood, so the accurate control of these process parameters is particularly important for the growth of high quality structures, declared Zhao, Chen and Wu [1]. For laser cladding, Kovacevic, Zhang and Li explained that the effect of these parameters on final products finally comes down to the temperature distribution, which greatly affects the shape of the melt pool [2]. That is, to some degree, the geometric stability of the melt pool indicates the microstructure stability of the products. Melt pool size is a key process characteristic that must be controlled to allow the precise deposition of complex features. An understanding of transient changes in melt pool size is important to control melt pool size in real time, via thermal imaging or other feedback control systems.

Meanwhile, interaction between the laser and the powder particles leads to attenuation of the laser and makes the powder particles' temperature rise, even melt. Several mathematical models have been established for simulating and predicting the formation of various microstructures. To the author's knowledge, little information is available in literature about models for predicting and controlling the cross sectional area of coaxial laser cladding with powder. Zhang studied the relationship between the cross sectional area and the multiple process parameters [3]. However, his study focused on the lateral supply of powder (off-axial powder injection).

In this paper, a vision-based sensing and control system is developed to detect the geometric parameters of the melt pool, and a mathematical model is presented to describe the interaction between laser and powder particles and to study the cross sectional area of coaxial laser cladding with powder injection. The experiments are carried out with alloy powder Ni60 and a CO<sub>2</sub> laser as heat source.

## 2. Experimental setup

The experiments were conducted on the close-loop controlled laser cladding system, which consists of four units: 3.0 KW CO<sub>2</sub> laser, 5-axis CNC machine, powder-feeder subsystem and monitoring subsystem.

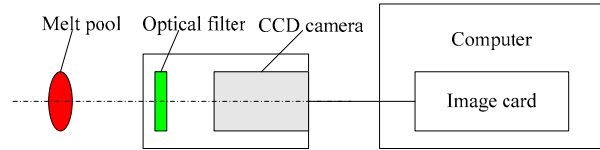


Figure 1. Experimental apparatus and setup

### Nomenclature

$A$	absorptivity of laser beam on metal surface
$C$	specific heat capacity (J/(kg·°C))
$C_z$	concentration of traveling powder cloud (kg/m <sup>3</sup> )
$G$	acceleration of gravity (m/s <sup>2</sup> )
$h$	height of nozzle (m)
$I_0$	initial laser power intensity (W/m <sup>2</sup> )
$I_a$	absorbed power intensity (W/m <sup>2</sup> )
$I_t$	transmitted power intensity (W/m <sup>2</sup> )
$I_r$	reflected power intensity (W/m <sup>2</sup> )
$l$	effective laser path length (m)
$m$	mass of melted powder particles (kg)
$P$	laser power (W)
$Q_1$	energy powder particles absorbed (J)
$Q_2$	laser energy absorbed by powder particles (J)
$r_p$	mean radius of powder particles (m)
$R_l$	radius of laser beam (m)
$R_p$	radius of focused powder stream (m)
$S$	cross sectional area (m <sup>2</sup> )
$t$	interaction time of laser beam and metal powders (s)
$T_0$	preheat temperature (°C)
$T_f$	final temperature (°C)
$T_m$	melting point of the powder particles (°C)
$V_0$	powder flow speed (m/s)
$V_f$	powder feed rate (kg/s)
$V_s$	scan speed (m/s)
$\Delta T$	temperature difference (°C)
$\Delta H$	latent heat of fusion (J/kg)

### Greek symbols

$\varepsilon$	absorption coefficient
$\eta$	efficiency of laser-material interaction (%)
$\theta$	angle of incidence (rad)
$\rho$	density (kg/m <sup>3</sup> )

Under the high-temperature condition, the melt pool may be regarded as the grey body. Non-contact measurement will be used to monitor the melt pool. In order to eliminate the infection of the measure distance and the material emission we use colorimetric technique to obtain the 2D temperature distributions of the melt pool. The melt pool is sensed by a high frame-rate (up to 100 frames per second) camera installed at the side of laser head, which takes grey images with a 640×480 resolution. The infrared radiation from the melt pool forms an image on the CCD chip of the camera (Figure 1).

## 3. Mathematical model

In this section, mathematical models are used to calculate the parameters of the melt pool and the cross sectional area.

### 3.1. Parameters of the melt pool

When the intense laser beam irradiates on the substrate surface, the melt pool will appear beneath the laser beam and it moves along with the motion of the laser beam. In order to interpret the geometry properties of the melt pool, computational domain in this study includes the geometry parameters, such as the pool width, length and rear angles. The governing equations can be expressed in the following form:

$$y_r = \pm ax_r^b (1 - x_r)^c, \quad (1)$$

where  $a = W_t / L_t$ ,  $x_r = x / L_t$ ,  $y_r = y / L_t$ .

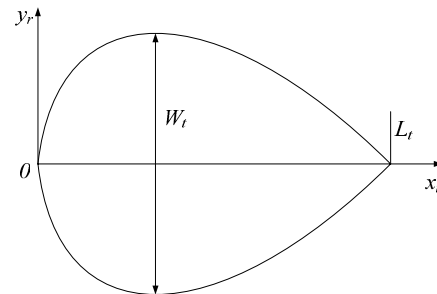


Figure 2. Melt pool parameters

### 3.2. Cross sectional area

A schematic presentation of coaxial powder injection is shown in Figure 3.

The model is based on the following assumptions:

- (i) The powder particles are spherical with properties not depend on temperature and the interaction between them is neglected.
- (ii) The powder particles are transported by the gravitation to the substrate.
- (iii) The energy intensity across the laser beam in which the powder particles travel is uniform. The laser beam can be seen as a cylinder

because of the high focal length compared with the radius of the laser beam.

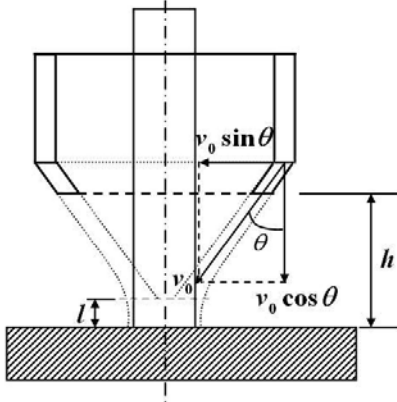


Figure 3. Coaxial powder injection

The cross sectional area of coaxial laser cladding is analysed by assuming for simplicity that all the powder particles have the same heating process  $T_0 \rightarrow T_m \rightarrow T_f$ .

After the heating process, the temperature of the powder particles reached at  $T_f$ . This process needs energy given by the following expression:

$$\begin{aligned} Q_1 &= mC(T_f - T_0) + m\Delta H \\ &= m(C\Delta T + \Delta H) \end{aligned} \quad (2)$$

The laser energy absorbed by the powder particles during the interaction time  $t$  is

$$Q_2 = \eta Pt, \quad (3)$$

where  $\eta$  is the efficiency of laser-material interaction which represents the percentage of energy absorbed by powder particles with respect to energy exported by laser beam. According to the law of conservation of energy,  $Q_1$  equals  $Q_2$ , which yield the following relationship between  $m$  and  $P$ :

$$\eta Pt = m(C\Delta T + \Delta H). \quad (4)$$

It can be solved to obtain

$$m = \eta P / (C\Delta T + \Delta H). \quad (5)$$

Since the length of scan line in unit time is equal to scan speed  $V_s$ , the cross sectional area  $S$  can be given by the following expression:

$$S = m / (\rho V_s) = \eta P / (\rho V_s (C\Delta T + \Delta H)). \quad (6)$$

The initial laser powder intensity  $I_0$  can be divided into three parts:  $I_a$ ,  $I_t$  and  $I_r$ , that is

$$I_0 = I_a + I_t + I_r. \quad (7)$$

According to the Beer-Lambert Law, the transmittance is given by

$$I_t / I_0 = \exp(-\varepsilon l C_z). \quad (8)$$

Here  $\varepsilon$  is absorption coefficient, which depends on the wave length of the laser beam and physical property of the metal powders.

Time during which powder particles moves from the nozzle to the surface of the substrate is:

$$t_1 = 2h / \sqrt{v_0^2 \cos^2 \theta + 2gh} + v_0 \cos \theta. \quad (9)$$

Similarly, time cost from the nozzle to the position where powder particles focus can be given by the following expression:

$$t_2 = 2(h-l) / \sqrt{v_0^2 \cos^2 \theta + 2g(h-l)} + v_0 \cos \theta. \quad (10)$$

Thus, interaction time  $t$  can be given by  $t = t_1 - t_2$ .

Since  $l$  is small, the focused powder stream is columnar. Therefore, concentration of the travelling powder cloud  $C_z$  is expressed as

$$C_z = V_f (t_1 - t_2) / (\pi R_p^2 l). \quad (11)$$

Substituting  $C_z$  from equation (11) into equation (8), the transmittance can be shown to be

$$I_t / I_0 = \exp(-\varepsilon V_f t / (\pi R_p^2)). \quad (12)$$

At certain wavelength of the laser beam, for CO<sub>2</sub> laser, which is 10.6 $\mu$ m, absorption coefficient  $\varepsilon$  can be estimated using the following experience-formula:

$$\varepsilon = 3(1-A) / (2r_p \rho), \quad (13)$$

where  $r_p$  presents the mean radius of powder particles. Near the melting point of the metal particles,  $A \approx 0.9$ . So  $\eta$  can be given by

$$\begin{aligned} \eta &= (1 - I_t / I_0) A \\ &= (1 - \exp(-3V_f t (1-A) / (2\pi r_p R_p^2))) A \end{aligned} \quad (14)$$

Substituting  $\eta$  from equation (14) into equation (6), the cross sectional area  $S$  is rewritten by the following expression:

$$S = \frac{P(1 - \exp(-3V_f t (1-A) / (2\pi r_p R_p^2))) A}{\rho V_s (C\Delta T + \Delta H)}. \quad (15)$$

#### 4. Results and discussion

The image acquiring system obtains 256-color grey scale bitmaps and sends them to the image processing module, which then calculates the geometric parameters and shows them in a real-time curve on the computer screen. Figure 4 (upper left) shows the experimental observation acquired by the CCD camera from the top of the melt pool.

With the captured images of the melt pool, the shape parameters of the melt pool can be calculated to meet the requirement of real time feedback by using an image processing method. The digital image processing method is an accurate, quick and direct

measure of the geometric parameter of the melt pool and its stability as well.

The algorithm takes the following steps (Figure 4. The lower right one gives the profile of the melt pool.):

- 1) Noise reduction;
- 2) Segmentation;
- 3) Profile fitting;
- 4) Measuring.

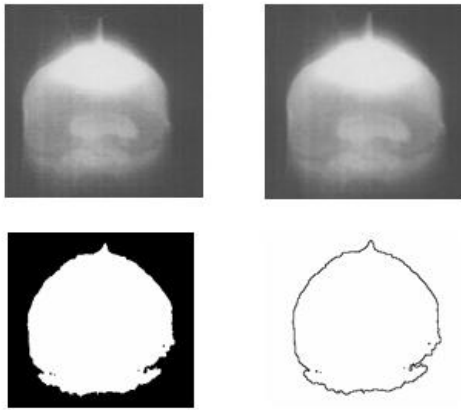


Figure 4. Image processing steps

The physical properties of the material Ni60 is shown in Table 1, and the experimental parameters are initialized (Table 2) and adjusted during the experiment. Figure 5 shows the sample formed in the experiment. We can see the sample has well geometrical accuracy and surface finish.

Table 1. Physical properties of Ni60

$C$ (J/(kg·°C))	$\Delta H$ (J/kg)	$\rho$ (kg/m <sup>3</sup> )	$r_p$ (m)	$A$
$0.464 \times 10^3$	$0.248 \times 10^6$	$8.522 \times 10^3$	$0.074 \times 10^{-3}$	0.9

Table 2. The experimental parameters

$P$ (W)	$V_s$ (mm/s)	Spot diameter (mm)
1000	3	0.9

## 5. Conclusions

Relationship between the geometry properties and the process parameters has been established. The results show good agreement with the computational data that the variation of laser power, powder feed rate, scan speed play significant roles on heat dissipation and the melt pool shape

This system gives us the necessary tools to gain insight into the cladding process and optimize material quality.



Figure 5. A sample formed in the experiment

A mathematical model is developed to analyze laser-material interaction and the effects of process parameters on the cross sectional area of coaxial laser cladding. According to this model, the cross sectional area can be determined computationally. Correlations between main process parameters and geometrical characteristics of an individual laser track have been found. The model should be useful in selecting process parameters, thus reducing the amount of experiments and their costs.

## 6. References

- [1] D.B. Zhao, S.B. Chen, and L. Wu, Shape Parameter Definition and Image Processing of the Weld Pool during Pulsed GTAW with Wire Filler. *Transaction of the China welding institution*, 2001, 22(2), pp. 5-8.
- [2] R. Koyacevic, Y.M. Zhang, and L. Li, Monitoring of weld joint penetration based on weld pool geometrical appearance. *Welding Journal*, 1996, 75, pp. 32-36.
- [3] Q.M. Zhang, An investigation on the applying fundamentals of powder feeding laser cladding, Ph.D. Thesis, 2000.
- [4] Y.C. Fu, A. Lored, B. Martin, and A.B. Vannes, A theoretical model for laser and powder particles interaction during laser cladding, *Journal of Material Processing Technology*, 2002, 128, pp. 106-112.
- [5] D.M. Hu, R. Kovacevic, Sensing, modeling and control for laser-based additive manufacturing, *Machine Tools and Manufacture*, 2003(43), pp. 51-60.

## Acknowledgement

Many thanks are due to my dear teacher John Paddison for his valuable suggestions and to Fei Xing for assistance with the experimental setup in this work.